Available online at www.sciencedirect.com
ScienceDirect
Polymer 48 (2007) 5174–5180
polymer
www.elsevier.com/locate/polymer

Diffusivity of *n*-hexane in poly(ethylene-*stat*-octene)s assessed by molecular dynamics simulation

A. Mattozzi, M.S. Hedenqvist, U.W. Gedde*

School of Chemical Science and Engineering, Fibre and Polymer Technology, Royal Institute of Technology, SE-100 44 Stockholm, Sweden

Received 26 February 2007; received in revised form 11 June 2007; accepted 16 June 2007
Available online 27 June 2007

Abstract

Molecular dynamics simulations have been used to study diffusion of *n*-hexane in wholly amorphous poly(ethylene-*stat*-octene)s with comonomer contents ranging from 0 to 11.5 mol%. The branches in the polymer increased the specific volume by affecting the packing of the chains in the rubbery state in accordance with experimental data. The diffusion of *n*-hexane at penetrant concentrations between 0.5 and 9.1 wt% was simulated within time-scales between 0.1 and 0.2 μs. The penetrant diffusivity unexpectedly decreased with increasing comonomer content. The penetrant molecule motion statistics showed that systems with high comonomer content showed a greater tendency for short distance motion (over a sampling period of 3 ps) whereas the systems with lower comonomer content showed penetrant motion over longer distances. It seems that the branches retarded local chain mobility of the polymer thereby trapping the penetrant molecules. All systems studied showed a minimum in penetrant diffusivity at ca. 1 wt% *n*-hexane and a marked increase in diffusivity at higher penetrant concentrations. The volumetric data for the different polymer–penetrant systems were consonant with additional volumes of the different components. Comparison between simulated diffusivities (for a wholly amorphous polymer) and experimentally obtained diffusivity data for semicrystalline polymers showed that constraining effect of the crystals were substantial for the highly crystalline systems and that it gradually decreased with decreasing crystallinity.

Keywords: Poly(ethylene-*stat*-octene); *n*-Hexane; Molecular dynamics simulation

1. Introduction

The transport of small molecule penetrants through a polymer is controlled by several factors: penetrant molecule size, affinity of penetrant to polymer, polymer free volume, crystal morphology and crystallinity [1,2]. The development of metallocene catalysts has led to the synthesis of homogeneous ethylene-α-olefin copolymers with narrow molar mass distributions and an almost uniform distribution of comonomers within and among different polymer molecules permitting the production of low crystallinity polyethylene with a relatively narrow crystal thickness distribution and narrow melting range. The authors have reported experimental data on the diffusive behaviour of *n*-hexane in a series of homogeneous poly(ethylene-*co*-octene)s with different comonomer contents, specifically relating crystal morphology and phase composition and amorphous fractional free volume and geometrical impedance factor [3,4]. The zero-concentration penetrant diffusivity in the liquid-like component was assumed constant and independent of the comonomer content in this analysis. It has been shown that the hexyl branches in poly(ethylene-*co*-octene) are confined to the amorphous component [5–7]. The nature of the amorphous component is expected a priori to depend on the concentration of hexyl branches. This study was aimed to reveal whether the *n*-hexane diffusivity in the liquid-like amorphous component of polyethylene depends on the branch content. Other issues dealt with were the volume additivity of penetrant and polymer, the concentration dependence of the penetrant diffusivity and the relationship between the diffusivities obtained by simulation and the experimentally

* Corresponding author. Tel.: +46 8 7907640; fax: +46 8 208856.
E-mail address: gedde@polymer.kth.se (U.W. Gedde).

0032-3861/$ - see front matter © 2007 Elsevier Ltd. All rights reserved.
doi:10.1016/j.polymer.2007.06.051

determined diffusivities for semicrystalline poly(ethylene-*co*-octene)s.

Molecular dynamics simulation has proven to be an effective method alternative to experimental techniques for estimating a variety of properties of dense polymers [8–10]. The diffusion of small gas penetrant molecules in solid and molten polymers has been studied by molecular dynamics simulation [8,11–13]. Molecular dynamics simulation is capable of studying wholly amorphous systems at temperatures well below the equilibrium melting point even in the case of readily crystallizable polymers like polyethylene [11,12,14,15]. The structure and properties of the amorphous component of polyethylene are in practice strongly influenced by the crystalline phase [3,4,16–18] and the properties of the isolated amorphous component can only be captured by indirect methods or by extrapolation from the melt. Analysis of the diffusive process for larger molecules, like the one used in this study (*n*-hexane), requires an adequate extension of the length- and time-scales of the simulated system. The use of an efficient algorithm and a state-of-art hardware permits the study of systems of up to 8000 atoms on a 4 μs time-scale [19].

In the present study the diffusion of *n*-hexane in five poly(ethylene-*stat*-octene)s with different comonomer content, has been studied by molecular dynamics simulation (NVT dynamics) for time-scale up to 0.2 μs. All systems were equilibrated using NPT dynamics before the assessments of the penetrant trajectories. The diffusion of *n*-hexane has been assessed for different penetrant concentrations ranging from 0.46 to 9.1 wt%.

2. Simulation details

2.1. System representation

The polymer systems studied contained five chains, each consisting of 1000 backbone carbon atoms. Repeating units based on 1-octene were randomly inserted into the chains obtaining the following systems with different comonomer contents (given in mol%; the sample codes are displayed within the parentheses): 0 (PE), 0.96 (EO1.0), 2.68 (EO2.7), 5.92 (EO5.9) and 11.52 (EO11.5). The number of carbon atoms of the different systems studied ranged from 5000 for PE to 6728 for the system with the highest comonomer content (EO11.5). In addition, the systems also contained *n*-hexane penetrant molecules in amounts corresponding to the following approximate mass percentages: 0, 0.5, 1, 2, 4 and 9. The methylene and methyl groups in both the polymer chains and in the penetrant molecules (*n*-hexane) were represented as anisotropic united atoms [20]. The carbon and hydrogen atoms of the CH– groups of the branching units were represented explicitly. The simulated systems were subjected to rectangular periodic boundary conditions.

2.2. Molecular dynamics details

The simulations were carried out using the GROMACS package [21] on several Nocona-Xeon®-equipped workstations. Constant pressure and temperature dynamics were obtained by a weak coupling to a pressure and temperature bath with coupling times of 1.5 ps (pressure) and 0.5 ps (temperature) according to the method of Berendsen et al. [22]. The time step was set to 1 fs for simulation establishing the PVT relationships and to 2 fs for the assessments of the penetrant trajectories.

All the boxes were obtained by placing the five polymer chains and the penetrant molecules in all-trans conformation in a very large periodic box, allowing each box to shrink in steps at high temperature under constant particle number, pressure and temperature (NPT) dynamics until the size of the box was stabilized. The systems were finally cooled to 298.15 K and equilibrated at this temperature during a time period of 10 ns after which the volume constancy was controlled. The equilibrium was assumed to be attained when the volume fluctuations were within 1% of the mean value for a time period of minimum 1 ns. If this condition was not fulfilled, the system was again equilibrated during an additional time period of 10 ns, and the volume constancy was again controlled during the subsequent 1 ns. PVT data covering the temperature range 298.15 K–550 K were obtained by successive heating and volume equilibration under isothermal conditions (NPT dynamics) in accordance with the aforementioned method.

2.3. Potential functions

The potential function parameters used in the simulations are presented in Table 1 and they were obtained from Pant et al. [23]. The truncation distance for non-bonded interactions was set to 1 nm.

2.4. Diffusion of n-hexane

Penetrant molecule trajectories were recorded under constant particle number, volume and temperature (NVT) dynamics for 0.1–0.2 μs after establishing volumetric equilibrium

Table 1
Potential functions for linear polyethylene and poly(ethylene-*stat*-octene)s[a]

Function	Constants		
Bond stretch energy $= k_R(R - R_0)^2/2$			
C–C	$k_R = 663$		$R_0 = 1.54$
C–H	$k_R = 663$		$R_0 = 1.54$
Bond angle bending energy $= k_\theta(\theta - \theta_0)^2/2$			
$-CH_2-$	$k_\theta = 482$		$\theta_0 = 111.6$
$>C<$	$k_\theta = 482$		$\theta_0 = 109.47$
Torsional potential $= V_3(1 + \cos 3\phi)/2$		$V_3 = 13.4$	
Non-bonded potential $= 4\sum_{i<j} \varepsilon_{ij}[(\frac{\sigma_{ij}}{r_{ij}})^{12} - (\frac{\sigma_{ij}}{r_{ij}})^{6}]$			
$-CH_2-$ (AUA)	$\varepsilon = 0.686$	$\sigma = 3.510$	$d = 0.42$
C (in $>CH-$)	$\varepsilon = 0.397$	$\sigma = 3.450$	$d = 0$
H (in $>CH-$)	$\varepsilon = 0.041$	$\sigma = 3.00$	$d = 0$
$-CH_3$ (AUA)	$\varepsilon = 0.837$	$\sigma = 3.763$	$d = 0.42$

[a] Data according to Pant et al. [23]. Energies are provided in kJ mol^{-1}, distances are given in Å and angles in radians. Parameters in the non-bonded potential function were calculated from the values given for individual atoms (or AUA) by taking the geometrical mean values (ε_{ii}) and the arithmetic mean values (σ_{ij}) of the interacting atoms. The parameter d is the offset distance (in Å) of the interaction centre from the carbon atom along the bisector C–C–C angle in the direction of the hydrogen atoms.

of the polymer–penetrant system under NPT dynamics (see Section 2.2). Each polymer system (five included in the study) was tested with five different penetrant concentrations ranging from ca. 0.46 to 9.1 wt%. After each simulation the volumetric invariance of the system was checked using NPT dynamics during a time period of 10 ns. The penetrant diffusivity (D) was determined according to the Einstein equation [24] from the mean square displacement $r(t)$ of the centre-of-mass of the penetrant molecule at time t from the origin $r(0)$:

$$D = \frac{\langle (r(t) - r(0))^2 \rangle}{6t} \quad (1)$$

The averaging was done by generating a new origin at every sampled point along the penetrant trajectory.

3. Results and discussion

3.1. PVT behaviour

The importance of obtaining realistic PVT properties for the host polymer in diffusion studies has been underlined in several molecular dynamics simulation studies [11,25]. The specific volumes of linear polyethylene and of the four poly(ethylene-*stat*-octene)s studied at different temperatures and normal pressure are shown in Fig. 1 together with experimental data on linear and branched polyethylene presented by Olabisi and Simha [26]. The difference between the simulated and experimental data in the molten state (>420 K) at normal pressure were ca. 2%, which is in accordance with earlier data presented by Karlsson et al. [15] using the same force fields (Fig. 1). In addition, the difference in specific volume between linear and branched (ca. 2 mol% branches corresponding to ca. 4 mol% comonomer units) polyethylene in the molten state according to data presented by Olabisi and Simha [26] was on an average 0.5%, which is of the same order of magnitude as obtained for the simulated structures. The anisotropic united atom potentials used in this study provide according to Pant et al. [23] a realistic static structure for linear polyethylene expressed in terms of PVT data and the radial distribution function.

Fig. 2 shows that the specific volume at room temperature and normal pressure increased linearly with increasing comonomer content according to the simulations. The specific volume value obtained by simulation for linear polyethylene at 298.15 K and normal pressure was 1.171×10^{-3} m^3 (kg)$^{-1}$, which is very close to the values obtained by extrapolation of experimental data, 1.170×10^{-3}–1.171×10^{-3} m^3 (kg)$^{-1}$ [27,28]. A value for the specific volume of the amorphous component for a poly(ethylene-*co*-octene) with 10.2 mol% 1-octene was calculated from data of Neway et al. [4]. This polymer had a specific volume of 1.164×10^{-3} m^3 (kg)$^{-1}$. Raman spectroscopy data analyzed according to Mutter et al. [29] showed the following phase composition of this particular sample: 0.85 (liquid-like), 0.137 (interfacial crystal core), 0.013 (interfacial liquid-like) and 0.00 (crystal core, i.e. orthorhombic crystal). A comprehensive set of data for poly(ethylene-*co*-octene)s [4,30] including data for specific volume (v), mass fractions of the crystal core component (w_{CC}), liquid-like component (w_L) and the two interfacial components (interfacial crystal core (ICC) and interfacial liquid-like (IL); $w_I = w_{ICC} + w_{IL}$) was used to calculate the specific volume of the interfacial component (v_I):

$$v_I = \frac{v - v_{CC}w_{CC} - v_L w_L}{w_I} \quad (2)$$

where v_{CC} is the specific volume for the crystal core component (1.004×10^{-3} m^3 (kg)$^{-1}$ [31]) and v_L is the specific volume of the liquid-like component; values were obtained from the data obtained by molecular dynamics simulation presented in Fig. 2. Fig. 3 shows that the specific volume of the interfacial component depends strongly on the overall specific volume (i.e. crystallinity). The following specific volume of the interfacial component corresponding to a specific volume of

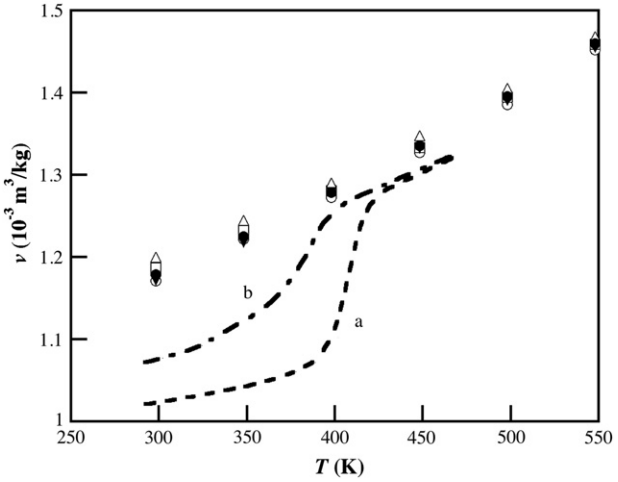

Fig. 1. Specific volume (v) at 10^5 Pa as a function of temperature (T) for PE (○), EO1.0 (▼), EO2.7 (●), EO5.9 (□), and EO11.5 (△). Experimental data from Olabisi and Simha [26] are shown for linear polyethylene (line a) and branched polyethylene (line b).

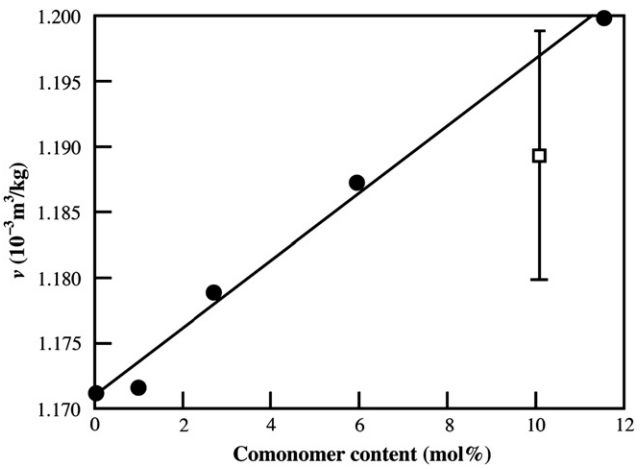

Fig. 2. Specific volume (v) at 298.15 K and 10^5 Pa as a function of comonomer content. Data represented by filled circles are from MD simulations and the open square represents a data point obtained by extrapolation of the experimental data displayed in Fig. 3.

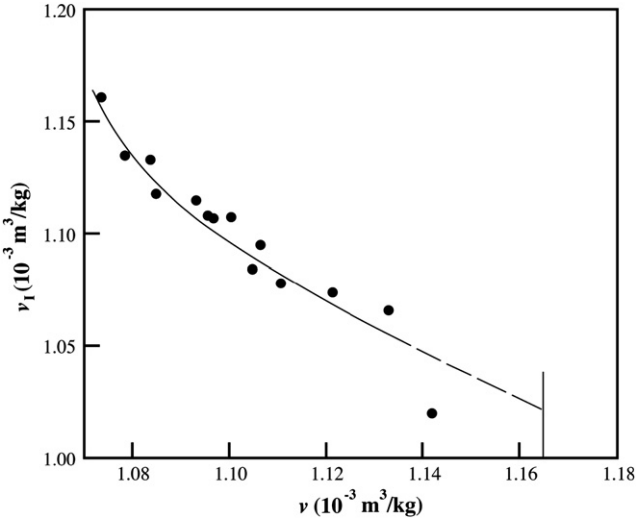

Fig. 3. Specific volume of interfacial component (v_I) as a function of specific volume (v) of semicrystalline polymer at room temperature and normal pressure. Calculated from data of Neway et al. [4,30].

1.164×10^{-3} m^3 $(kg)^{-1}$ was obtained by extrapolation (Fig. 3): $1.020 \pm 0.010 \times 10^{-3}$ m^3 $(kg)^{-1}$. The interfacial component consists, according to Mutter et al. [29], of chain segments with a conformation different from that typical of the liquid-like component, rich in trans-conformers but lacking orthorhombic packing. Thus it means that this component in principle could contain a variety of structures, i.e. monoclinic crystals, hexagonal phase and amorphous chains with special conformation. Lagaron [32] reported the presence of small crystals of non-orthorhombic packing in very low-density polyethylene. Androsch et al. [33,34] observed in a poly(ethylene-*co*-octene) with 7.3 mol% octene a Bragg reflection corresponding to a *d*-spacing that could be assigned to either a monoclinic phase or a hexagonal phase. McFaddin et al. [35] reported the presence of monoclinic crystals (specific volume at room temperature: 1.002×10^{-3} m^3 $(kg)^{-1}$ [36]) in similar polymers. The systematic change in v_I with crystallinity (specific volume) displayed in Fig. 3 suggests that the nature of the interfacial phase is gradually changing with crystallinity and that for the very low crystalline polymers, such as the one with a specific volume of 1.164×10^{-3} m^3 $(kg)^{-1}$, it is dominated by monoclinic and/or hexagonal phases. The calculated liquid-like component density of the polymer (with 10.2 mol% comonomer and a specific volume of 1.164×10^{-3} m^3 $(kg)^{-1}$) became $1.189 \pm 0.010 \times 10^{-3}$ m^3 $(kg)^{-1}$, which, by considering the relatively low precision in the calculation, is in accordance with the data obtained by simulation (Fig. 2). The relatively large uncertainty in the determination (± 0.010 m^3 $(kg)^{-1}$) has two sources: (i) extrapolation of the specific volume data of the interfacial component (± 0.010 m^3 $(kg)^{-1}$); (ii) assessment in the phase composition of the poly(ethylene-*co*-octene) with 10.2 mol% 1-octene, ± 0.03.

3.2. Penetrant diffusion

The mean square displacement plot of *n*-hexane, averaged for five molecules, in linear polyethylene is shown in Fig. 4a. The initial part of the plot, including the first 100 ns, is linear; the slope was used as the input for the assessment of the penetrant diffusivity according to Eq. (1). The average displacement of an individual *n*-hexane molecule was ca. 7 nm over a period of 100 ns, i.e. 13 times the end-to-end distance of *n*-hexane (0.54 nm) at 298.15 K according to a calculation by Monte Carlo simulation. Fig. 4b shows the logarithm of the square displacement as a function of the logarithm of time and the fact that the slope is linear and near unity (1.05) between 10 and 100 ns confirmed that the system reached the diffusive regime [37].

The effect of polymer branching on the low penetrant concentration diffusivity is displayed in Fig. 5. Unexpectedly, the presence of branches decreased the diffusivity in the simulated systems regardless of the fact that it increased the specific volume (cf. Figs. 2 and 5). Hence, the polymers with high comonomer content exhibited a high average free volume but evidently the branches, being the reason for the volumetric

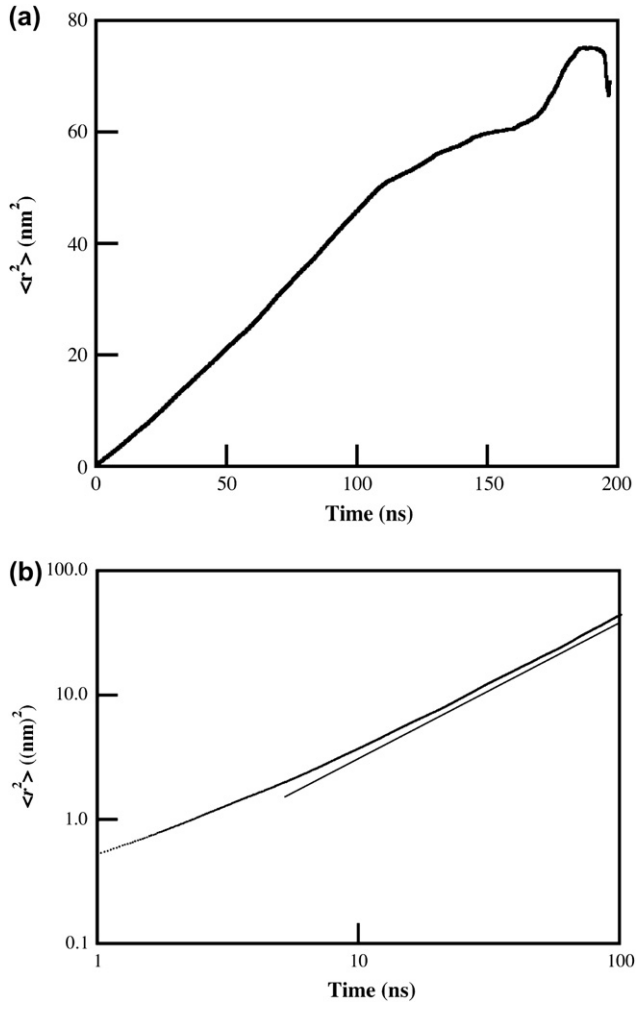

Fig. 4. (a) Mean square displacement ($\langle r^2 \rangle$) of the centres of mass of five molecules of *n*-hexane in linear polyethylene as a function of time. (b) Mean square displacement (logarithmic scale) ($\langle r^2 \rangle$) as a function of time (logarithmic scale) for *n*-hexane in polyethylene. Calculated from the data presented in Fig. 4a. The straight line is added to help the eye to identify the linear regime.

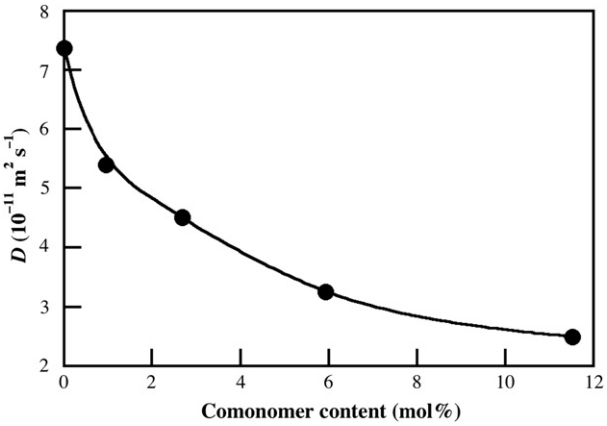

Fig. 5. *n*-Hexane diffusivity (D) at low penetrant concentration (ca. 0.5 wt%) as a function of comonomer content for simulated systems.

effect, also acted as traps for the penetrant molecules. The segmental mobilities of the backbone segments nearest to the branch points should be reduced; this supposition finds some grounding in molecular dynamics simulation studies [38] of branched systems. The observed decrease in diffusivity with increasing comonomer content was further validated by a study of the penetrant molecule centre-of-mass motion statistics (Fig. 6a and b)). The peaks appear at very short distances, ca. 0.03 nm. This means that the most typical captured motion is essentially within the cage of the surrounding molecules. The distributions were narrower in systems with higher comonomer content (Fig. 6a). In order to quantify the peakedness of the curves, the kurtosis was calculated for the given centre-of-mass jump length distributions (Fig. 6b): the high values of kurtosis for highly branched systems are due to a penetrant motion that is characterized by a high mobility on short length-scales and lower mobility on longer length-scales.

The *n*-hexane diffusivity in all the systems, assessed for varying penetrant contents, is shown in Fig. 7. The effect of branching in lowering the diffusivity is observed throughout the penetrant concentration range. All the systems showed a minimum in diffusivity at ca. 1 wt% penetrant concentration. The system with penetrant concentrations greater than 1 wt% showed an approximately exponential increase in diffusivity with increasing penetrant concentration (Fig. 7). The unexpected minimum in penetrant diffusivity at 1 wt% *n*-hexane content can tentatively be ascribed to the penetrant molecules that fill pre-existing free volume cavities in the polymer. However, the specific volume data shown for the polymer–penetrant systems studied provided no basis for this assumption (Fig. 8). The experimental data scatter around the line prescribed by constant mixing volume of the two components. The average deviation of individual simulated data points and the line was 0.5% of the absolute specific volume value, which is in accordance with the approval criterion for volumetric equilibrium (Section 2.2). It may thus be concluded that the volumetric data obtained by molecular dynamics simulation, admittedly with a significant degree of scatter (±0.5%), are in accordance with constant volume of mixing ($\delta V_{\mathrm{mix}} = 0$).

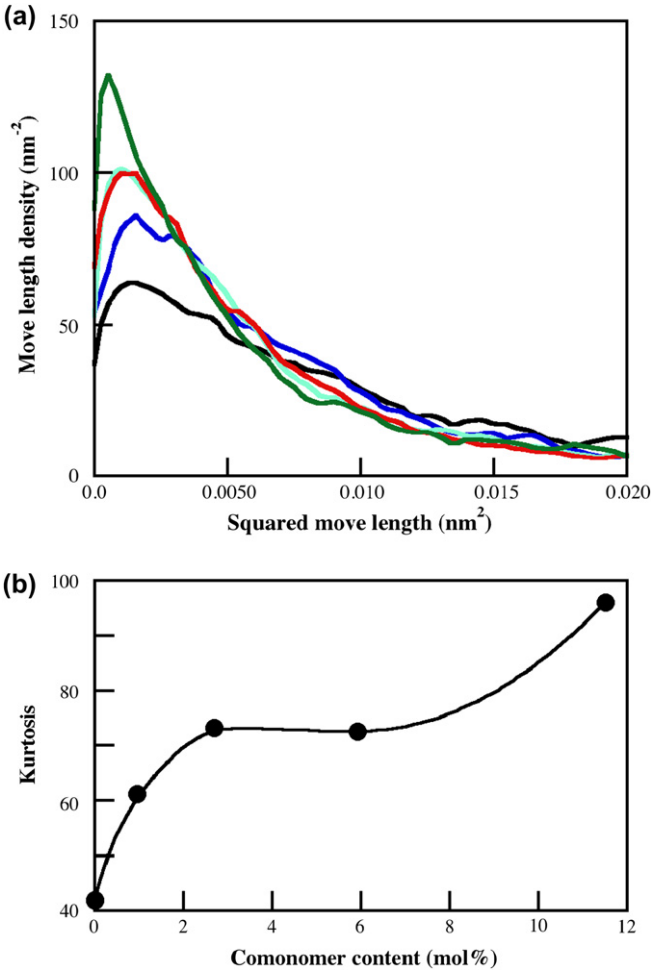

Fig. 6. (a) Distributions of moves of *n*-hexane centre-of-mass in PE (black), EO1.0 (blue), EO2.7 (light blue), EO5.9 (red), EO11.5 (green) with 0.5 wt% penetrant. The averaging time period was 3 ps. (b) Kurtosis of the distributions of penetrant moves presented in Fig. 6a as a function of comonomer content (for interpretation of the references to colour in this figure legend, the reader is referred to the web version of this article).

The minimum in diffusivity at ca. 1 wt% penetrant cannot be explained by a corresponding variation in the specific volume of the systems. The scatter in the specific volume of

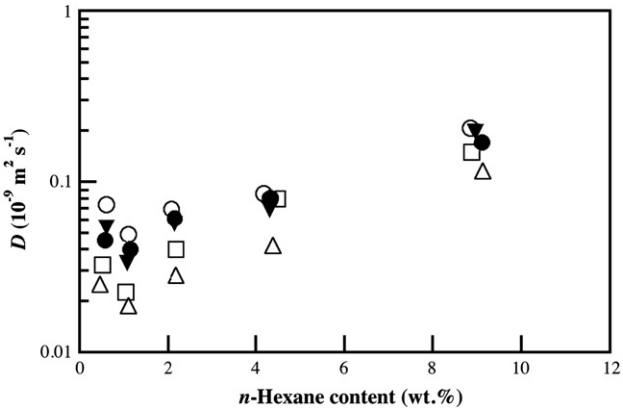

Fig. 7. *n*-Hexane diffusivity (D) as a function of *n*-hexane concentration for PE (○), EO1.0 (▼), EO2.7 (●), EO5.9 (□), EO11.5 (△).

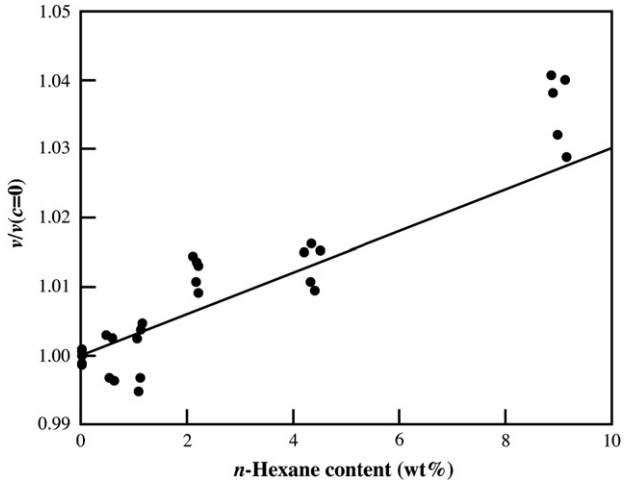

Fig. 8. Normalised specific volume (the ratio of the specific volume of the actual system (v) and the specific volume of the system at 0% penetrant concentration ($v(c=0)$) of polymer/*n*-hexane system at 298.15 K and 10^5 Pa as a function of *n*-hexane content. The continuous line represents the systems with constant volume of mixing.

individual polymer–penetrant systems with respect to the line prescribed by constant volume of mixing had essentially no impact on the penetrant diffusivity (cf. Figs. 7 and 8). The anomalous minimum in diffusivity at 1 wt% penetrant concentration shows some similarity with systems showing dual mobility: traps are filled with penetrant first and these molecules have a relatively low mobility; at higher penetrant concentration the 'matrix' is populated with more mobile penetrant molecules. It should be noted that both linear polyethylene and the branched polyethylenes showed essentially the same characteristic behaviour and thus the traps are not only associated with the chain branches.

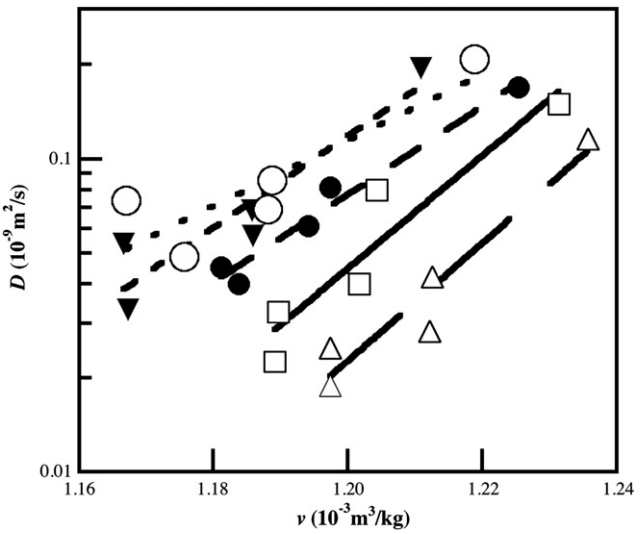

Fig. 9. Diffusivity of *n*-hexane (D) as a function of specific volume (v) of the system polymer/*n*-hexane for PE (○), EO1.0 (▼), EO2.7 (●), EO5.9 (□), and EO11.5 (△). The lines represent an exponential fit to the data obtained by simulation.

An empirical relationship was found between the *n*-hexane diffusivity in the polymer and the density of the system (Fig. 9). It suggested that the diffusivity in a given polymer could be predicted from the specific volume of the polymer–penetrant system. However, the specific volume was proven to play a secondary role when comparing different polymers with different comonomer contents; in this case the molecular architecture played an important role.

Fig. 10 presents a comparison between penetrant diffusivity in the liquid-like component ($D_{L,0}$; curve (a)), data obtained by simulation (at 0.46 wt% *n*-hexane) in wholly amorphous polymer systems and experimental zero-concentration diffusivity (D_0; curve (b)), data for semicrystalline poly(ethylene-*co*-octene)s earlier reported by Neway et al. [4]. The relationship between two diffusivities can be expressed according to Michaels and Bixler [16]:

$$D_0 = \frac{D_{L,0}}{\tau \times \beta} \tag{3}$$

where τ is the geometrical impedance factor and β is the immobilization factor which takes into account the constraining effect of the crystals on the amorphous component. Curve (c) in Fig. 10 represents $D_0\tau = D_{L,0}/\beta$; the geometrical impedance factors for the different samples were calculated from the morphological data of Mattozzi et al. [3] using an equation derived by Michaels and Bixler [16] based on the Fricke theory [39]. Fig. 10 shows that $D_0 \ll D_{L,0}$ and $\beta \gg 1$ for the polymers with low comonomer contents. There is a gradual decrease in the constraining factor (β) with increasing

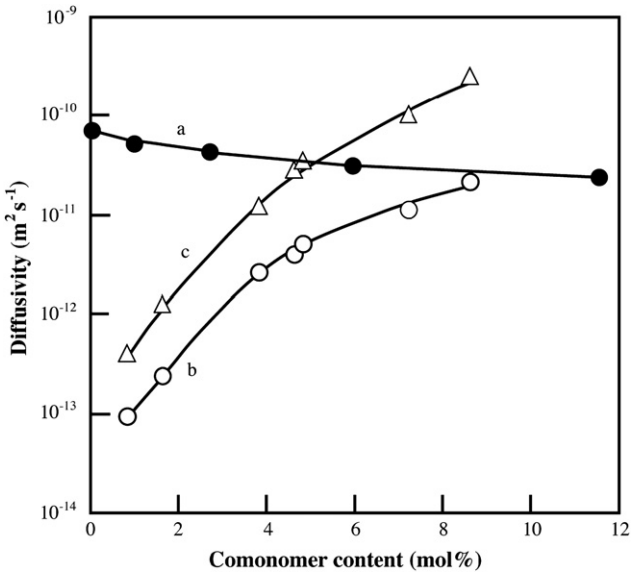

Fig. 10. Diffusivity of *n*-hexane as a function of comonomer content for the following systems: (a) by molecular dynamics simulation in wholly amorphous polymer with 0.46 wt% *n*-hexane ($D_{L,0}$); (b) zero-concentration diffusivity (D_0) calculated from experimental desorption data on semicrystalline poly(ethylene-*co*-octene)s reported by Neway et al. [4]; (c) zero-concentration diffusivity (D_0) according to (b) multiplied with the geometrical impedance factor (τ) calculated according to the Fricke equation using morphological data by Mattozzi et al. [3].

comonomer content (decreasing crystallinity). Fig. 10 even shows that $D_0\tau = D_{L,0}/\beta > D_{L,0}$, i.e. $\beta < 1$. This unrealistic feature is due to lack of precision in the assessment of the different diffusivities and morphologically controlled geometrical impedance factor. The data showed, however, clearly the gradual change in β from a value close to 100 for the highly crystalline systems to values approaching unity (order of magnitude) for polymers with low crystallinity.

4. Conclusion

A series of poly(ethylene-*co*-octene)s with different comonomer contents ranging from 0 to 11.5 mol% was studied by molecular dynamics simulation. The specific volume increased with increasing comonomer content in accordance with experimental data. The hexyl branches evidently disturbed efficient packing of the amorphous polymer chains. The *n*-hexane diffusivity at low penetrant concentration decreased with increasing comonomer content. This was unexpected in view of the increase in specific volume with increasing comonomer content. The penetrant molecules showed fast local motion in the highly branched systems and, in a comparison with systems with fewer branches, fewer motions on a longer length-scale. All the systems showed a minimum in diffusivity at ca. 1 wt% penetrant concentration and at higher penetrant concentration a more expected approximately exponential increase in the diffusivity with increasing penetrant concentration. The observed minimum in diffusivity is remarkable in view of the specific volume data for the penetrant-polymer systems; the latter obeyed, within the precision of the molecular dynamic simulation method used, volume additivity of the individual constituents. A comparison between obtained simulated diffusivities and experimentally determined diffusivities showed that the constraining effect of the crystals on the non-crystalline components was very large for highly crystalline systems and that it gradually decreased with decreasing crystallinity.

Acknowledgements

The financial support from the Swedish Research Council (grant # 5104-20005764/20) is gratefully acknowledged. Drs. G.E. Karlsson and B. Neway are thanked for valuable discussions. The Centre for Parallel Computer (PDC) and the Swedish National Infrastructure for Computing (SNIC) are thanked for providing computing resources and support.

References

[1] Hedenqvist M, Gedde UW. Prog Polym Sci 1996;21:299.
[2] Vieth WR. Diffusion in and through polymers. Munich: Hanser Verlag; 1991.
[3] Mattozzi A, Neway B, Hedenqvist MS, Gedde UW. Polymer 2005; 46:929.
[4] Neway B, Westberg A, Mattozzi A, Hedenqvist MS, Baschetti MG, Mathot VBF, et al. Polymer 2004;45:3913.
[5] Hay JN, Zhou XQ. Polymer 1993;34:1002.
[6] Hosoda S, Nomura H, Gotoh Y, Kihara H. Polymer 1990;31:1999.
[7] Mathur SC, Mattice WL. Macromolecules 1987;20:2165.
[8] Müller-Plathe F. Acta Polym 1994;45:259.
[9] Fossey SA. In: Brostow W, editor. Performance of plastics. Munich, Cincinatti: Hanser Verlag; 2000 [chapter 2].
[10] Brostow W, Simoes R. J Mater Ed 2005;27:19.
[11] Han J, Boyd RH. Macromolecules 1994;27:5365.
[12] Pant PVK, Boyd RH. Macromolecules 1993;26:679.
[13] Gusev AA, Müller-Plathe F, van Gunsteren WF, Suter UW. Adv Polym Sci 1994;116:209.
[14] Boyd RH, Gee RH, Han J, Jin Y. J Chem Phys 1994;101:788.
[15] Karlsson GE, Johansson TS, Gedde UW, Hedenqvist MS. Macromolecules 2002;35:7453.
[16] Michaels AS, Bixler HJ. J Polym Sci 1961;5:393.
[17] Boyd RH. Polym Eng Sci 1979;19:1010.
[18] Fleischer G. Coll Polym Sci 1984;262:919.
[19] Karayiannis NC, Mavrantzas VG. Macromolecules 2005;38:8583.
[20] Toxvaerd SJ. J Chem Phys 1990;93:4290.
[21] Van Der Spoel D, Lindahl E, Hess B, Groenhof G, Mark AE, Berendsen HJC. J Comput Chem 2005;26:1701.
[22] Berendsen HJC, Postma JPM, van Gunsteren WF, Di Nola A, Haak JR. J Chem Phys 1984;81:3684.
[23] Pant PVK, Han J, Smith GD, Boyd RH. J Chem Phys 1993;99:597.
[24] Einstein A. Ann Physik 1905;17:549.
[25] Van der Vegt NFA. Macromolecules 2000;33:3153.
[26] Olabisi O, Simha R. Macromolecules 1975;8:206.
[27] Allen G, Gee G, Wilson GJ. Polymer 1960;1:456.
[28] Wunderlich B. Crystal structure, morphology, defects. In: Macromolecular physics, vol. 1. New York and London: Academic Press; 1973. p. 388.
[29] Mutter R, Stille W, Strobl G. J Polym Sci Part B Polym Phys 1993;31:99.
[30] Neway B, Hedenqvist MS, Mathot VBF, Gedde UW. Polymer 2001;42:5307.
[31] Busing WR. Macromolecules 1990;23:4608.
[32] Lagaron JM. Macromol Symp 2002;184:19.
[33] Androsch R, Blackwell J, Chvalun SN, Wunderlich B. Macromolecules 1999;32:3735.
[34] Androsch R, Wunderlich B. Macromolecules 2000;33:9076.
[35] McFaddin DC, Russell KE, Wu G, Heyding RD. J Polym Sci Part B Polym Phys 1993;31:175.
[36] Clark ES. In: Mark JE, editor. Physical properties of polymers handbook. Woodbury, New York: American Institute of Physics; 1996. p. 410.
[37] Hofmann D, Fritz L, Ulbrich J, Schepers C, Bohning M. Macromol Theory Simul 2000;9:293.
[38] Jabbarzadeh A, Atkinson JD, Tanner RI. Macromolecules 2003;36:5020.
[39] Fricke H. Phys Rev 1924;24:575.